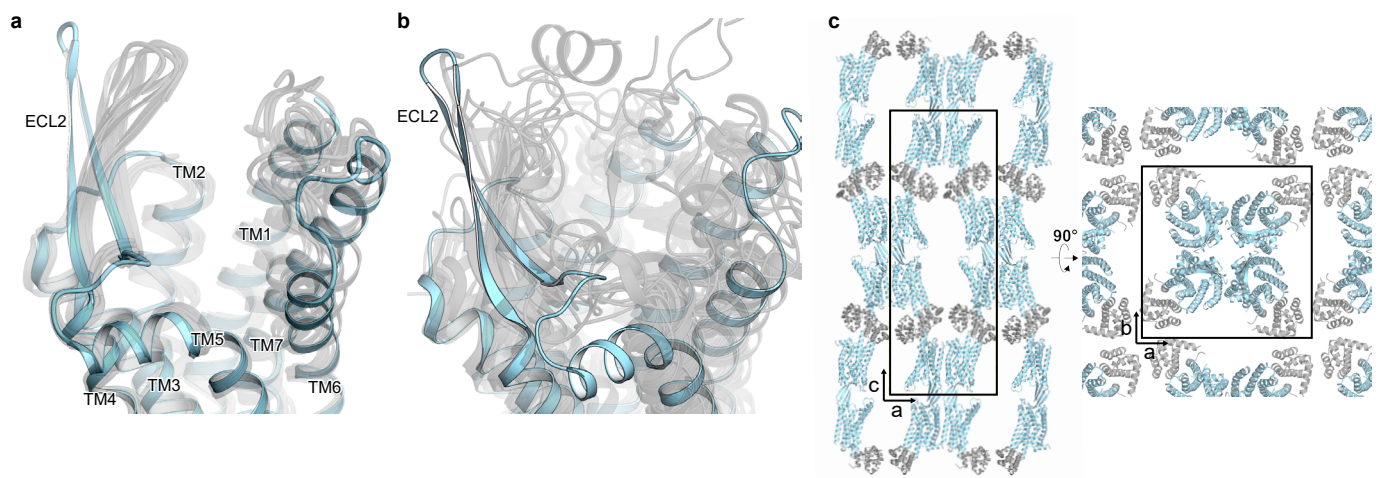


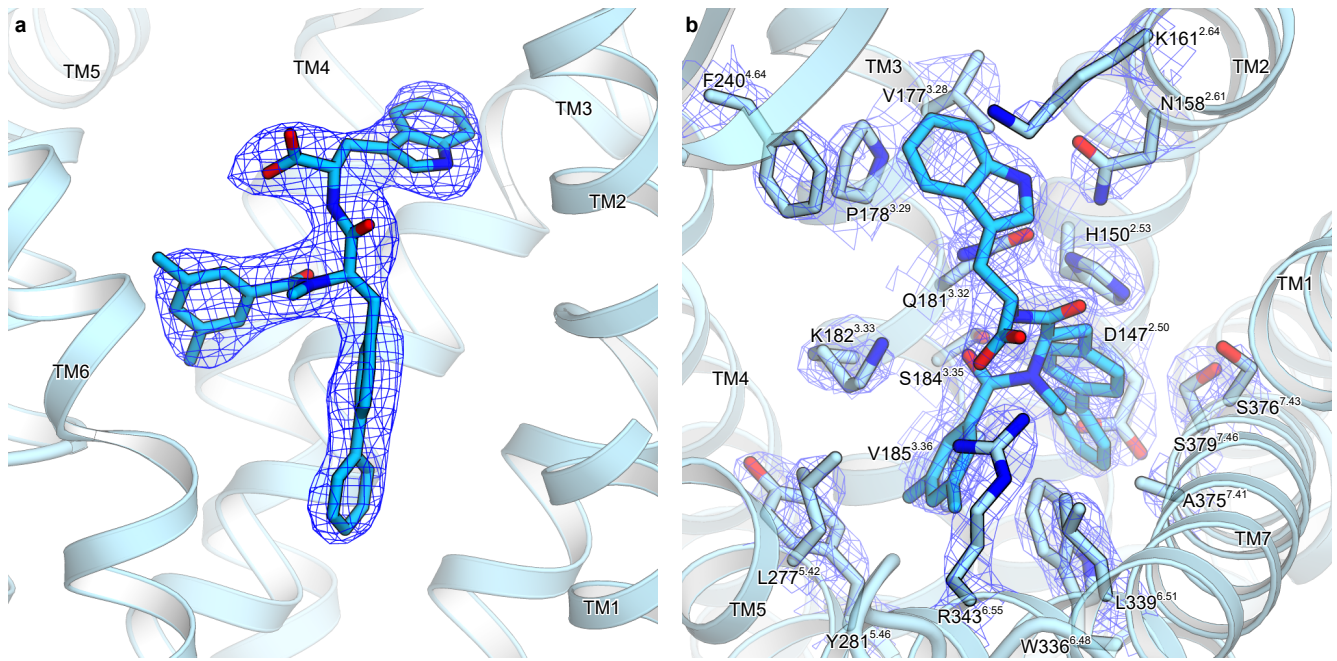
Supplementary Figure 1 | Crystallization.

a, Gel filtration chromatogram and SDS-PAGE of the purified IRL2500-bound ET_B receptor. **b**, Crystals of the IRL2500-bound ET_B receptor.



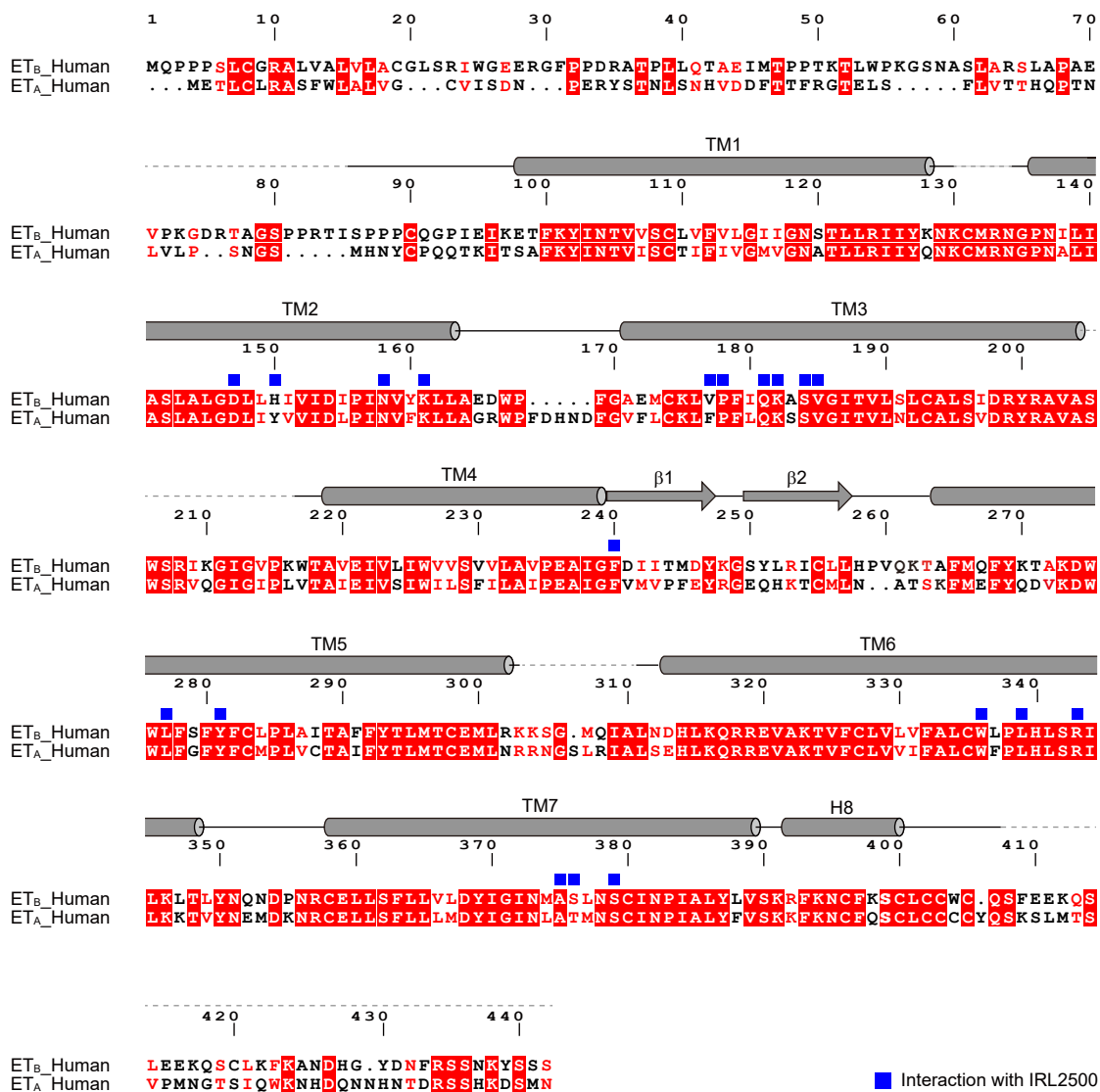
Supplementary Figure 2 | Comparison of the ECL2 structure with those of other peptide-activated GPCRs.

a, Superimposition of the ET_B structures determined to date. The IRL2500-bound and other structures are coloured sky blue and gray, respectively. **b**, Superimposition of the IRL2500-bound ET_B structure with other peptide-activated class A GPCRs. **c**, Crystal packing of the IRL2500-bound ET_B structure. The receptor and T4L are shown as grey and blue ribbons, respectively. The crystal lattice is indicated by black lines.



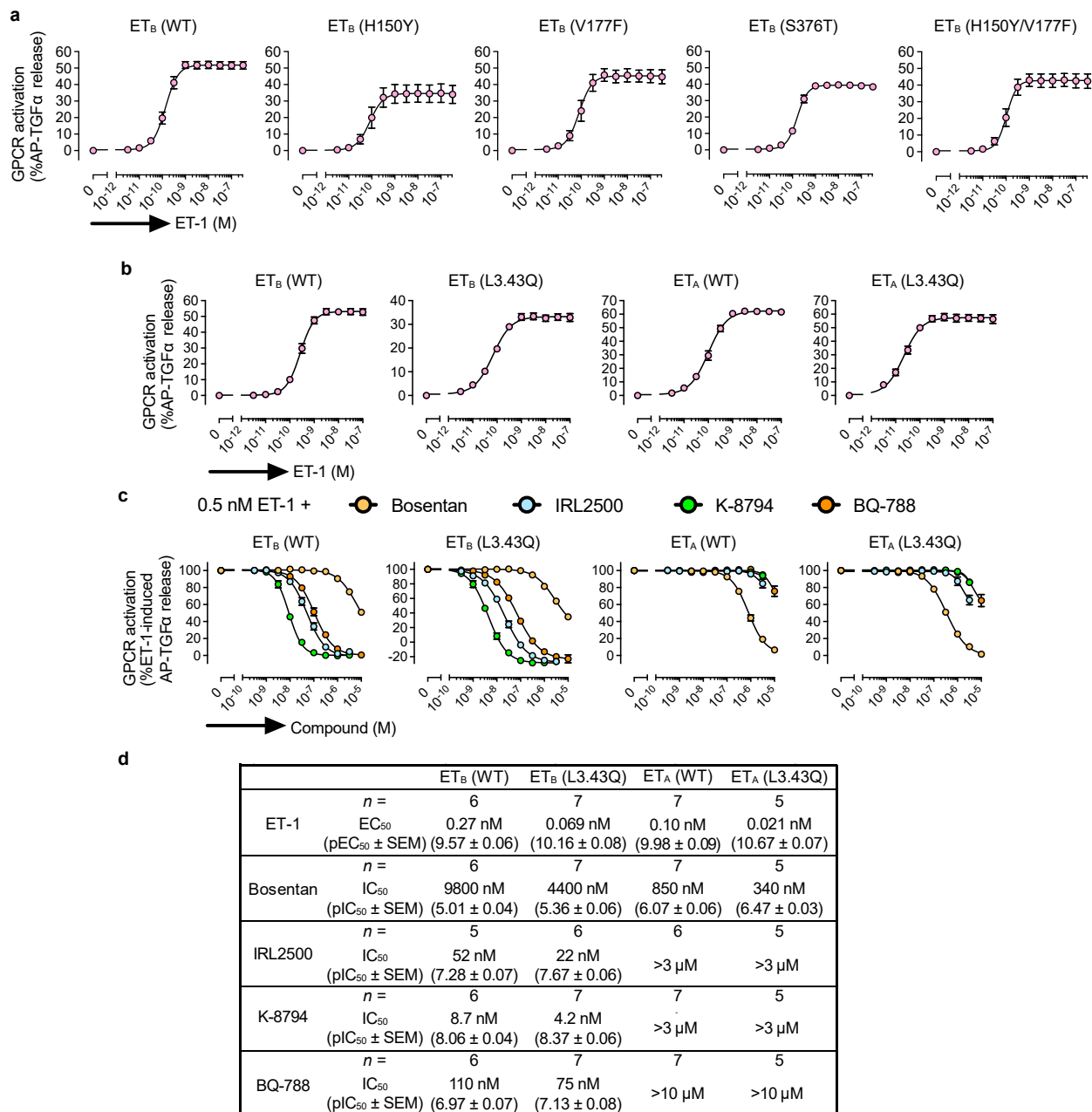
Supplementary Figure 3 | Electron density.

a, $F_o - F_c$ omit maps for IRL2500, contoured at 3.0σ . **b**, $2F_o - F_c$ map around the IRL2500 binding site, contoured at 2.5σ .



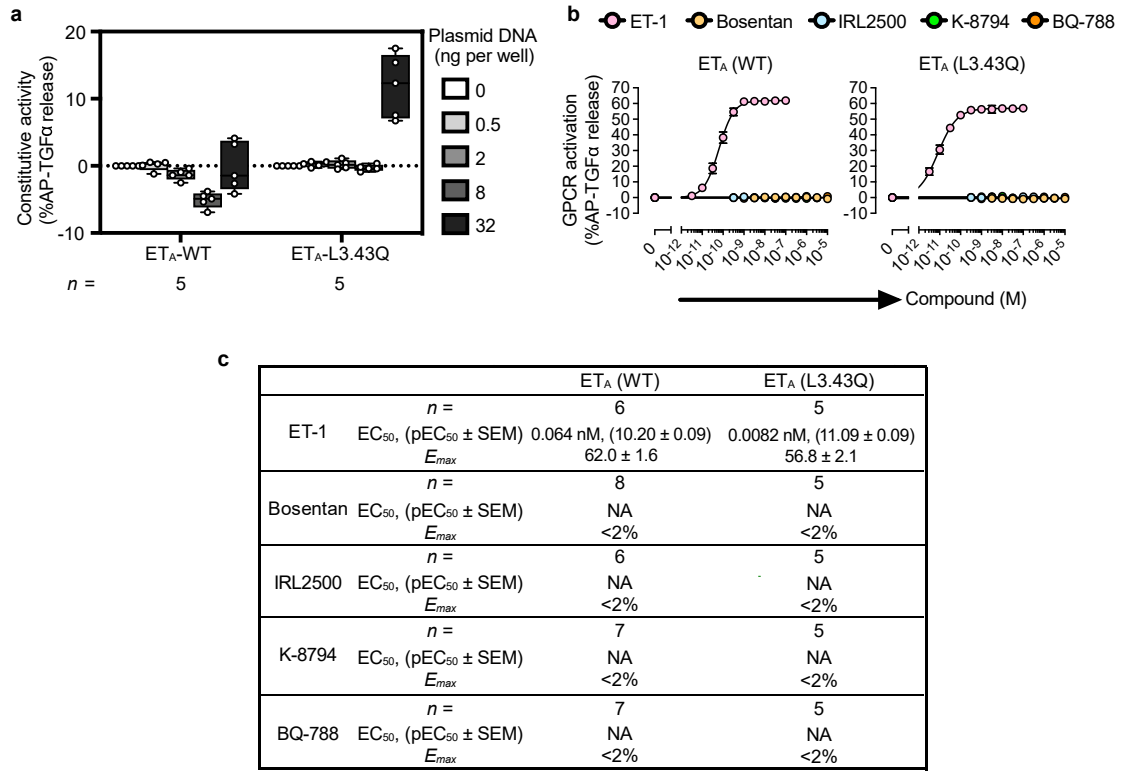
Supplementary Figure 4 | Alignment of the human ET_A and ET_B receptors.

Alignment of the amino acid sequences of the human ET_B receptor (Uniprot ID: P24530) and the human ET_A receptor (P25101). Secondary structure elements for α-helices and β-strands are indicated by cylinders and arrows, respectively. Conservation of the residues between ET_A and ET_B is indicated as follows: red panels for completely conserved; red letters for partially conserved; and black letters for not conserved. The residues involved in IRL2500 binding are indicated with squares.



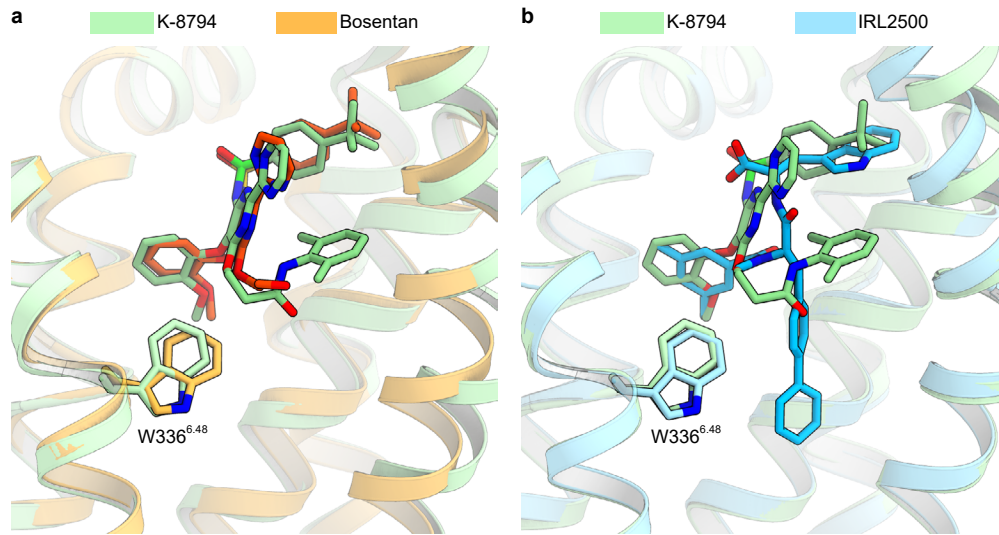
Supplementary Figure 5 | Pharmacological characterization of mutant receptors.

a, b, Concentration response-curves of AP-TGF α release in the ET-1 treatment of HEK293 cells expressing the mutant ET_B receptors (**a**) and the constitutively active L3.43Q-mutant receptors (**b**). Symbols and error bars are means and s.e.m. (standard error of the mean) of four to seven independent experiments, each performed in duplicate or triplicate. **c**, Effect of the antagonists on ET-1 (0.5 nM)-induced responses of AP-TGF α release in HEK293 cells expressing the wild-type or constitutively active endothelin receptors. For each experiment, the AP-TGF α release response in the absence of the antagonist is set at 100%. Data are displayed as means \pm s.e.m. (standard error of the mean) from five to seven independent experiments, with each performed in duplicate or triplicate. **d**, Parameters for the agonist and the antagonists. From the concentration-response curves in (**b**) and (**c**), pEC₅₀ values (ET-1) and pIC₅₀ values (antagonists) were calculated. Mean pEC₅₀ and pIC₅₀ values were used to calculate EC₅₀ and IC₅₀ values, respectively.



Supplementary Figure 6 | Characterization of inverse agonist activities for the ET_A receptors.

a, Constitutive activity of the L3.43Q-mutant ET_A receptors (ET_A-L3.43Q). HEK293 cells were transfected with a titrated volume of a plasmid encoding the wildtype ET_A (ET_A-WT) or the ET_A-L3.43Q and the accumulated AP-TGF α release during 24 h after transfection was measured. The AP-TGF α release signal in the 0 ng receptor plasmid was set as the baseline. **b**, **c**, Effects of ET-1 and the ET_B antagonists (bosentan, IRL2500, K-8794 and BQ-788) on the AP-TGF α release for the wild-type or constitutively active ET_A receptor (ET_A-L3.43Q). The cells were incubated with the compounds for 4 h, instead of 1 h, the condition that was used for the other antagonist experiments. For each experiment, the AP-TGF α release response in the absence of the compound is set at the baseline. Data are displayed as means ± s.e.m. from five to eight independent experiments.



Supplementary Figure 7 | Comparison of the K-8794, bosentan, and IRL2500-bound structures.
a,b, Superimpositions of the K-8794-bound receptor with the bosentan- (a) and IRL2500-bound receptors (b).